

## Density-dependent pair interactions in 2D colloidal suspensions

M. BRUNNER<sup>1</sup>(\*), C. BECHINGER<sup>1</sup>, W. STREPP<sup>1</sup>,  
V. LOBASKIN<sup>2</sup> and H. H. VON GRÜNBERG<sup>1</sup>(\*\*)

<sup>1</sup> *Fakultät für Physik, Universität Konstanz - 78457 Konstanz, Germany*

<sup>2</sup> *Institute of Physics, University of Fribourg - CH-1700 Fribourg, Switzerland*

PACS. 82.70.Dd – Colloids.

PACS. 05.40.-a – Fluctuation phenomena, random processes, noise, and Brownian motion.

PACS. 61.20.-p – Structure of liquids.

**Abstract.** – We experimentally determine effective interparticle potentials in a two-dimensional (2D) colloidal system of charge-stabilized polystyrene particles at different particle densities  $\rho$ . Density variation is achieved by means of a scanned optical laser tweezer which serves to create a boundary box for the system. By changing the size of this boundary box,  $\rho$  can be systematically varied without having to prepare a new system. From the measured radial distribution functions we can then obtain the effective pair potentials of the particles. While for low particle densities perfect agreement with Yukawa-like potentials is observed, considerable deviations from this form are found at higher densities. We interpret this result as a many-body effect produced by macroion screening which is expected to become more pronounced as the density is increased.

There are several analogies between a charge-stabilized colloidal suspension and a fluid metal. A metal essentially consists of highly charged core ions plus the screening charge cloud of the electrons, which the ions are embedded in [1]. Colloidal suspensions, on the other hand, are composed of large and highly charged particles, *i.e.* macroions which are suspended in a structureless medium and surrounded by a screening atmosphere of microions. Common to both systems is that there are two classes of ingredients (ions/electrons and macroions/microions) which move and respond on totally separated length and time scales. Accordingly, similar theoretical concepts can be applied in both the theory of metals and that of colloidal suspensions. One of the major theoretical tasks in the description of metals is to reduce the many-body electron-ion Hamiltonian to an effective ionic Hamiltonian which is expressed as a sum of volume-, pair-, triple-, and multi-ion interactions. This can be achieved by eliminating the electronic degrees of freedom. In a similar manner, one of the fundamental questions in colloidal systems is, how to integrate out the microionic degrees of freedom and to calculate *effective* macroion/macroion forces, consisting of the direct Coulomb repulsions and an indirect interaction mediated by the small ions of the electrolyte. In contrast to fluid metal, however, a suspension of charged colloidal particles can directly be observed and studied under an optical microscope. Accordingly, colloidal suspensions provide an ideal testing ground for the various concepts to attack the interesting many-body problem. In the following, we will in particular focus on the widely used concept of “effective” pair interactions [2, 3].

---

(\*) E-mail: [Matthias.Brunner@uni-konstanz.de](mailto:Matthias.Brunner@uni-konstanz.de)

(\*\*) E-mail: [Hennig.vonGruenberg@uni-konstanz.de](mailto:Hennig.vonGruenberg@uni-konstanz.de)

In case of colloidal systems, many-body effects are encountered because the interaction between macroions strongly depends on the distribution of the screening electrolyte ions and thus implicitly on the macroion density  $\rho$ . In other words, a variation of  $\rho$  does not only affect the mean distance between macroions, but also changes the form of the effective pair potentials, hence  $u(r; \rho)$ . This density-dependence of  $u(r; \rho)$  is more than a trivial dependence on some additional parameter; it expresses the fact that, in principle, higher-order contributions, such as three-body potentials between the colloids, have to be taken into account which are now partly incorporated in  $u(r; \rho)$  [1]. The importance of a density-dependent pair potential on, *e.g.*, the phase behavior of a system becomes immediately obvious if one considers the virial equation for  $\rho$ -dependent potentials [1],

$$\beta p = \rho - \frac{\beta \rho^2}{2} \int d\mathbf{r} g(r; \rho) \left( \frac{r}{3} \frac{\partial}{\partial r} - \rho \frac{\partial}{\partial \rho} \right) u(r; \rho), \quad (1)$$

where  $g(r; \rho)$  is the pair distribution function,  $\beta = 1/kT$  with  $k$  the Boltzmann constant,  $T$  the temperature and  $p$  the pressure. While the first and second term in eq. (1) are standard terms accounting for the ideal gas behavior and the pairwise interaction between the particles, the third term  $-\rho \partial u(r; \rho) / \partial \rho$  arises due to the density dependence of  $u(r; \rho)$  and can be viewed as an additional force acting on the particles. It is negative if the pair potential becomes increasingly repulsive with growing density, and may thus produce a van-der-Waals-like instability even in fluids with purely repulsive pair potentials [4]. It can also lead to a second liquid-liquid phase separation in systems that already show a gas-liquid phase-coexistence [5].

Several experiments have been reported in the literature [6–9], where interaction potentials of colloids in suspensions were measured. Most of them were performed in 2D systems because the reduction to 2D allows the convenient determination of colloidal positions by means of video microscopy. From these positions one can directly obtain the structure in colloidal fluids, *i.e.* the radial pair distribution function (RDF)  $g(r; \rho)$ , and from it effective potentials  $u(r; \rho)$ . We here follow the previous studies in that we investigate a 2D suspension of charged colloids to measure effective potentials in the way just described; the new aspect of this paper, however, is that the focus lies on the density-dependence of  $u(r; \rho)$ . We report on a systematic experimental investigation to study the question, if and beyond which value of  $\rho$  the density dependence of  $u(r; \rho)$  becomes important. As pointed out above, the onset of such a density-dependence would indicate that, in principle, the concept of pairwise colloid-colloid interaction begins to become insufficient, as the influence of other colloids on the pair interaction becomes obviously non-negligible. In other words, a density-dependence of  $u(r; \rho)$  would be a clear fingerprint for the occurrence of many-body interactions. Such a study became possible through a well-controlled density variation by using a scanned optical tweezer to create and vary the boundary box confining the colloidal system under investigation. Our results clearly demonstrate that pronounced changes in  $u(r; \rho)$  occur at high particle densities; this underlines the importance of many-body interactions in such systems.

As colloidal system we used an aqueous suspension of highly charged sulphate-terminated PS particles of  $\sigma = 3 \mu\text{m}$  diameter with an average polydispersity below 4% (Interfacial Dynamics Cooperation). The attached surface groups are fully dissociated. The experimental set-up was composed of a silica glass cuvette with a 1 mm spacing, which was included into a closed water circuit to achieve the maximum de-ionization of the water. The circuit consisted of the sample cell, an electrical conductivity meter, a vessel of ion exchange resin, a reservoir basin and a peristaltic pump. Before the measurement, the water was highly de-ionized (corresponding to an ionic conductivity below  $0.07 \mu\text{S/cm}$ ) in the circuit. Only then the colloidal suspension was injected into the cell. The cell was sealed from the circuit during the

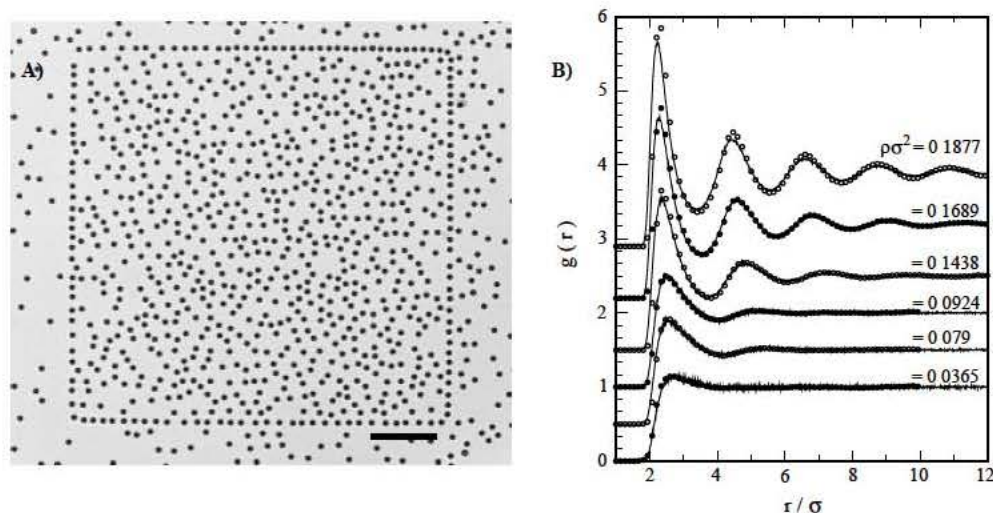


Fig. 1 – A) Optical image of the 2D colloidal suspension. 1D arrays of colloids whose positions are held fixed by light forces are used to realize a 2D colloidal system with a well-defined colloid density. The bar corresponds to  $50 \mu\text{m}$ . B) Radial distribution functions for the identical set of colloids inside the rectangular box depicted in A), for varying box sizes (*i.e.*, colloid densities  $\rho\sigma^2$ ). Symbols for the experimental data, solid lines for MC data. Note that the data have been shifted in vertical direction for clarity.

measurements. The high quality of the silica cell allowed us to keep the concentration of salt ions constant for over 24 hours [10]. The colloidal system was confined to two dimensions by a widened beam ( $500 \mu\text{m}$  HWHM) of  $0.4 \text{ W}$  of a frequency-doubled Nd:YVO<sub>4</sub> laser which was directed from above into the sample cell. The particles were thus exposed to vertical light forces which pushed them toward the negatively charged silica plate of the cell, confining the system effectively to two dimensions [11]. The particle center positions were analyzed on-line with an imaging processing software (Visiometrics, IPS). To ensure that the individual pictures are statistically independent only one picture per second was taken. In case of low particle densities up to 20000 pictures were recorded. The variation of the particle density was in our experiments achieved by a scanned optical laser tweezer which acts as a corral for the investigated 2D colloidal suspension. The beam of an Ar-ion laser was reflected from a 2D galvanostatic driven mirror and focused with a spot size of about  $2 \mu\text{m}$  into the sample plane. The mirror unit was controlled by a computer in such a way that the tweezer was repeatedly scanning a rectangular box. Since the repetition rate of about  $50\text{Hz}$  was much faster than typical relaxation times in the colloidal system, this resulted in a quasi-static optical trap for the colloidal particles along the contour of the box. The laser intensity was adjusted to about  $200 \text{ mW}$ , which corresponds to a potential depth in the order of about  $30 \text{ kT}$ . Accordingly, once a particle was entering the trap it was impossible for it to escape. As can be seen in fig. 1A, the particles arranged like a pearl-necklace along the contour of the laser trap and thus served —due to their electrostatic interaction— as a corral for the particles inside the box. By changing the size of the rectangular box, the density of the enclosed particles could be changed in a controlled manner and thus allowed us to measure the RDFs of an *identical* set of particles at different  $\rho$ . Figure 1B shows the measured RDFs for six different values of  $\rho\sigma^2$  between  $\rho\sigma^2 = 0.04$  and  $\rho\sigma^2 = 0.19$ , beyond which value the suspension starts to crystallize. The determination of the effective potentials from  $g(r)$  [13]

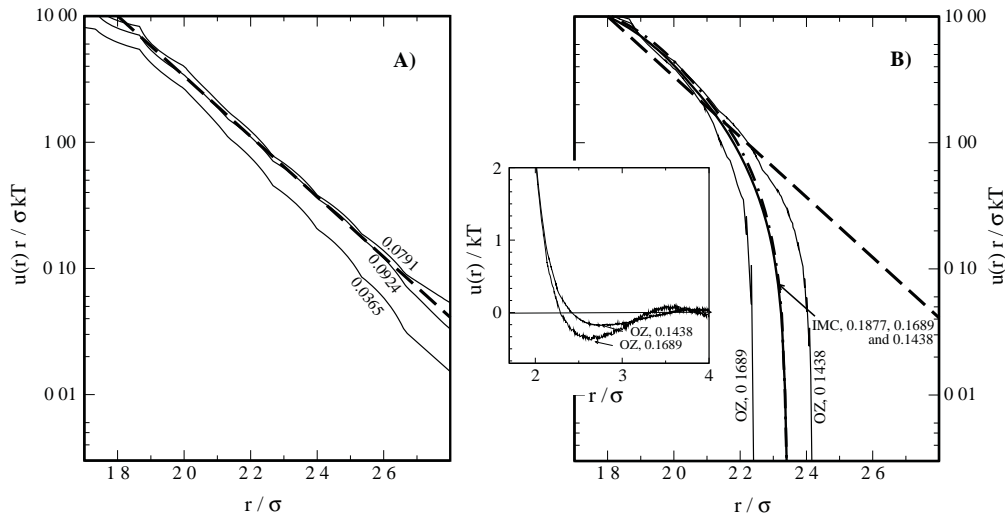


Fig. 2 – Effective colloid-colloid pair potentials, obtained from inverting the measured  $g(r)$  in fig. 1. Potentials are multiplied by  $r$  and plotted logarithmically, in A) for the three lowest and in B) for the higher colloidal densities. The thin solid lines are potentials obtained from an inversion method based on the Ornstein-Zernicke (OZ) equation (figures at the curve give the density  $\rho\sigma^2$ ). The thick dashed line is a reference Yukawa potential. The thick solid lines in B) are potentials obtained from an inverse Monte Carlo (IMC) procedure. The inset figure shows the potentials obtained from the OZ equation at larger distances.

proceeds as described, for instance, in ref. [8]. Calculating the fast Fourier transformation (FFT) of the total correlation function  $h(r) = g(r) - 1$ , we obtain  $\hat{h}(k) = \int d\mathbf{r} h(r) e^{-i\mathbf{k}\mathbf{r}}$  which is related to the Fourier transform of the direct correlation function  $c(r)$  via the Ornstein-Zernicke (OZ) equation,  $\hat{c}(k) = \hat{h}(k)/(1 + \rho\hat{h}(k))$ . With a FFT back to direct space, we arrive at  $c(r)$  which is connected to the pair potentials via the closure relations (CR). As CRs we use the hypernetted-chain (HNC)-, Percus-Yevick (PY)-, and mean-spherical approximation (MSA)-closure relation. Comparing the HNC-based potential with the one based on the PY-CR offers a way to keep control over the error produced by the inversion procedure. This inversion procedure was successfully tested by applying it to a RDF generated by a MC simulation of the system.

Figure 2 now shows the potentials obtained from the measured RDFs using the HNC-CR. In our experiment, the salinity is fixed to a  $\rho$ -independent value given just by the reservoir salinity. The reservoir is realized in our experiment by the electrolyte solution in the volume above the 2D colloidal system and the larger system of colloids outside the box, see fig. 1A. At fixed salinity the effective colloid-colloid potential in the classical DLVO theory [14, 15] (adapted using the concept of charge renormalization [16]) takes the form of a screened Coulomb potential,

$$\beta u(r) = \frac{Z_{\text{eff}}^2 \lambda_B}{(1 + \kappa\sigma/2)^2} \frac{\exp[-\kappa(r - \sigma)]}{r}, \quad (2)$$

with  $\lambda_B$  the Bjerrum length of the electrolyte solution, and  $Z_{\text{eff}}$  the effective charge [16].  $\kappa$  is given by  $\sqrt{8\pi\lambda_B c_s}$ , with  $c_s$  the reservoir salt concentration. This potential is the exact (within the mean-field approximation) long-distance asymptotic law for the potentials at infinite dilution in colloids, where “long-distance”  $D$  means  $\kappa(D - \sigma) \gg 1$ . To check if the

confinement by the charged glass plate has any effect on the pair potentials, we computed the pair interaction between two colloidal spheres in front of a charged wall from the solution of the full Poisson-Boltzmann equation, for the set of parameters realized in our experiment, and found no significant confinement effect [17]. So, eq. (2) should well describe the interaction of two colloids, even in our confined geometry.

In order to compare the obtained potentials with eq. (2), we multiplied  $u(r)$  by the radial distance and plotted the result logarithmically, so that Yukawa-like potentials must appear as straight lines. A look at fig. 2A reveals that for the three lowest densities considered, we indeed obtain potentials of an almost perfect Yukawa form, just as eq. (2) predicts. We note that all three curves have equal slope, meaning that the screening parameter  $\kappa$  is not changed upon changing the colloid density. Thus, the ( $\rho$ -independent) reservoir salt concentration  $c_s$ , not the local ( $\rho$ -dependent) concentration of microions determines the screening. This is an interesting result, containing another, less obvious piece of information. It is important to understand that the potential in eq. (2) is derived for two isolated colloids immersed in an infinite electrolyte of fixed salinity. It is obtained by first linearizing the Poisson-Boltzmann equation for the mean-field electrostatic potential  $\phi(r)$  of one colloid about zero potential, and by then superposing two such potentials for two colloids at a given distance [18]. At high colloid densities, this can fail because linearization about zero-potential is inappropriate. One can then try to linearize about the averaged potential (or the Donnan potential) in the suspension [19], resulting again in a Yukawa interaction potential, but now with a  $\kappa' = (4\pi\lambda_B(2n_s + n_c))^{1/2}$ , where  $n_s$  is the salt concentration inside the suspension ( $n_s \neq c_s$  because of the Donnan effect) and  $n_c$  is the  $\rho$ -dependent counterion concentration. The  $\kappa'$  thus obtained is much larger than the  $\kappa$  considered here. Our finding that  $\kappa$  remains constant for all densities considered thus implies that the averaged potential inside the suspension is still zero, and that the Donnan effect has not set in yet.

The vertical shifts of the curves in fig. 2A indicate a weak density dependence of the pre-factor of the effective Yukawa pair potential which reflects a slight change in the effective charge. This is consistent with earlier observations that the effective charge increases with density in this volume fraction interval [16]. We have fitted the  $\rho\sigma^2 = 0.0924$  curve to a function  $\beta u(r) = A\sigma \exp[-\kappa r]/r$ , obtaining  $A = 250000$  and  $\kappa\sigma = 5.5$  (thick dashed line in fig. 2A, B). This value corresponds to a screening length of  $\kappa^{-1} = 545$  nm. Using these values in a Yukawa interaction potential we performed standard MC simulations for a 2D Yukawa fluid at all six colloid densities investigated here and computed RDFs which we compare in fig. 1B with the experimental ones. As can be seen, for the three lowest densities the agreement is excellent.

For increasing density, however, the agreement between the experimental and numerical data in fig. 1B becomes systematically poorer; the MC simulation using the pair potential, eq. (2), slightly underestimates the structure. This already indicates that the potential (2) becomes inadequate at higher densities and must be corrected for many-body contributions. That rather small differences in  $g(r)$  can have large effects in  $u(r)$ , as is evident from fig. 2B showing the potentials at higher densities.  $u(r)$  is Yukawa-like only at very short distances, but shows significant deviations from the straight reference line for  $r > 2.1\sigma$ . The solid lines in the inset figure show the potential at higher distances. A very shallow minimum of 0.2 kT at  $\rho\sigma^2 = 0.1438$  and 0.5 kT at  $\rho\sigma^2 = 0.1689$ , which forms on increasing  $\rho$ , becomes visible. These deviations of  $u(r)$  from the Yukawa form, and in particular this minimum, are in striking contrast to the form of the potential in eq. (2), predicted by the DLVO theory. This is the more remarkable as one of the criteria for using eq. (2) should be well obeyed in our systems, since  $\kappa(D - \sigma) = 7.2 \gg 1$  with  $D = \rho^{-1/2}$  the mean distance at  $\rho\sigma^2 = 0.1877$ . We remark that a potential well of similar form and depth has also been observed in other 2D colloidal systems [8,9].

Before we give a physical interpretation of the observed deviations from the Yukawa po-

tential, we first want to discuss possible errors produced by the CRs which at high densities one would expect to fail. Indeed, at  $\rho\sigma^2 = 0.1689$ , the potentials obtained using the HNC-, PY- and MSA-CR already showed severe differences, which were in the order of the analyzed minima (though all three CRs produced attractive regions in the potentials!); at even larger densities,  $\rho\sigma^2 = 0.1877$ , the OZ-based inversion routine could no longer produce physically meaningful effective potentials. Therefore, we applied another, more rigorous procedure to invert the measured RDFs, *i.e.* the inverse Monte Carlo (IMC) method [20, 21], which was earlier successfully applied to charged colloids [22]. The main difference between the IMC and the OZ approach is that IMC uses a MC simulation instead of the approximative CRs to invert the RDFs, and hence should give a better solution of the inversion problem at higher densities. For the three lower volume fractions the IMC procedure resulted again in perfect Yukawa potentials (data not shown here) which are in good agreement with the three curves of fig. 2A. For the three higher densities ( $\rho\sigma^2 = 0.1438, 0.1689, 0.1877$ ), however, we found a strong density effect showing the same characteristic deviation from the Yukawa potential as the potentials based on the OZ inversion procedure, see fig. 2B. Because the three highest densities are very close to each other and because of a limited resolution of our IMC method, they only show small differences relative to each other and lie almost on top. In contrast to the OZ-based inversion procedure, no minimum is produced. We have found, however, that the potentials at larger distances depend on the chosen cut-off radius taken here to be  $4\sigma$ . Choosing a somewhat different cut-off radius, a shallow minimum (0.2 kT) was obtained also with the IMC procedure. We recognize that the uncertainty in the determination of the effective potential at larger separations (*i.e.* beyond the mean interparticle distance) is relatively high. The main figure of fig. 2B, however, reveals also— and that is the decisive point— that the IMC procedure confirms the deviation of the measured potentials from the Yukawa form (dashed thick line in fig. 2B) at  $r > 2.1\sigma$ . This feature remains regardless whether the true potential has a minimum or not.

Figure 2 thus demonstrates that two independent inversion procedures predict a non-trivial density-dependence of the effective pair potential, being Yukawa-like at low densities, but showing clear deviations from the expected Yukawa form at high densities. The fact that strong deviations of the measured potentials in fig. 2B take place at distances comparable to the mean colloid-colloid distance  $D = \rho^{-1/2}$  at the respective densities ( $D/\sigma = 2.3, 2.4, 2.6$  for the three highest densities and  $D/\sigma = 3.3, 3.5, 5.3$  for the three lowest colloid densities) suggests the following qualitative interpretation of our results: Two colloids in a suspension which are separated by  $r > D$  are likely to have a third particle somewhere in between. In contrast, the potential in eq. (2) is based on the assumption of two (and just two) interacting colloids, each surrounded by an unperturbed spherical double layer. This clearly cannot give the correct interaction potentials in cases where a third macroion in between is effectively blocking the mutual interaction of the two colloids. We call this effect macroion screening [23, 24]. Figure 2B is thus a direct experimental observation of many-body interactions in suspensions of charged colloids. This interpretation is also consistent with other experimental studies observing attractive parts in the colloid/colloid pair potential which were interpreted as “like-charge attraction” [7, 8]. Our results, however, suggest that this is a many-body contribution which when projected onto a pair potential can appear as a minimum, and can thus not be observed for an independent pair of particles.

\* \* \*

We thank R. KLEIN and P. LEIDERER for stimulating discussions, A. LYUBARTSEV for giving us access to his IMC code (VL) and the DFG for financial support (SFB 513/BE 1788/3 (CB)).

## REFERENCES

- [1] HAFNER J., *From Hamiltonians to Phase Diagrams* (Springer, Berlin, Heidelberg) 1987.
- [2] LÖWEN H. and HANSEN J. P., *Annu. Rev. Phys. Chem.*, **51** (2000) 209.
- [3] NÄGELE G., *Phys. Rep.*, **272** (1996) 215.
- [4] DIJKSTRA M. and VAN ROIJ R., *J. Phys. Condens. Matter*, **10** (1998) 1219.
- [5] ALMARZA N. G., LOMBA E., RUIZ G. and TEJERO C. F., *Phys. Rev. Lett.*, **86** (2001) 2038.
- [6] ATTARD P., *Curr. Opin. Colloid. Interfaces Sci.*, **6** (2001) 366.
- [7] VONDERMASSEN K., BONGERS J., MÜLLER A. and VERSMOLD H., *Langmuir*, **10** (1994) 1351; KEPLER G. M. and FRADEN S., *Phys. Rev. Lett.*, **73** (1994) 356; CARBAJAL-TINOCO M. D., CASTRO ROMAN F. and ARAUZ-LARA J. L., *Phys. Rev. E*, **56** (1996) 3745; BEHRENS S. H. and GRIER D. G., *Phys. Rev. E*, **64** (2001) 050401.
- [8] CRUZ DE LEÓN G. and ARAUZ-LARA J. L., *Phys. Rev. E*, **59** (1999) 4203.
- [9] QUESADA-PEREZ M., MONCHO-JORDA A., MARTINEZ-LOPEZ F. and HIDALGO-ALVAREZ R., *J. Chem. Phys.*, **115** (2001) 10897.
- [10] It is important to keep ion-exchange particles out of the sample cell. Even small ion-exchange particles can cause an enormous osmotic pressure, leading to non-equilibrium effects.
- [11] The Gaussian profile of the laser beam is expected to produce some gradient forces towards the center of the beam, which could lead to inhomogeneities in the particle density. Therefore the light intensity was chosen to be as low as possible and the beam was widened so much that the light intensity in the central region could be regarded as constant. That the system was homogeneous and not affected by the widened laser spot has been carefully and permanently checked by monitoring the 2D density distribution over the whole field of measurement. Since we did not observe any changes in the RDFs upon variation of the incident laser power, we rule out possible light-induced effects, such as optical binding [12].
- [12] BURNS M. M., FOURNIER J.-M. and GOLOVCHENKO J. A., *Phys. Rev. Lett.*, **63** (1989) 1233.
- [13]  $g(r)$  is obtained from  $\rho^2 g(r) = \langle \rho_N^2 g_N(r) \rangle$  with  $\rho = \langle \rho_N \rangle$  being the mean density and  $\rho_N(g_N(r))$  being the density (RDF) for a specific picture with  $N$  particles around a reference particle.
- [14] VERWEY E. J. W. and OVERBEEK J. T. G., *Theory of the Stability of Lyophobic Colloids* (Elsevier, Amsterdam) 1948.
- [15] EVANS D. F. and WENNERSTRÖM H., *The Colloidal Domain: Where Physics, Chemistry, Biology, and Technology Meet* (VCH, New York) 1994.
- [16] BELLONI L., *Colloids Surf. A*, **140** (1998) 227.
- [17] RUSS C., private communication.
- [18] BELL G. M., LEVINE S. and MCCARTNEY L. N., *J. Colloid Interface Sci.*, **33** (1970) 335.
- [19] VON GRÜNBERG H. H., VAN ROIJ R. and KLEIN G., *Europhys. Lett.*, **55** (2001) 580.
- [20] LOBASKIN V., LYUBARTSEV A. and LINSE P., *Phys. Rev. E*, **63** (2001) 020401.
- [21] R. L. HENDERSON, *Phys. Lett. A*, **49** (1974) 197.
- [22] LYUBARTSEV A. P. and LAAKSONEN A., *Phys. Rev. E*, **52** (1995) 3730; *Phys. Rev. E*, **55** (1997) 5689.
- [23] Of course, macroion screening occurs also in suspensions at lower densities, but for  $r > D$ , in these systems the pair potential has decayed essentially to zero.
- [24] In a numerical study, we have found that due to macroion screening the three-body contribution  $H_3$  in the total Hamiltonian  $H = H_1 + H_2 + H_3 + \dots$ , with  $H_1$  and  $H_2$  being the one- and two-body contributions, is always *negative*. Representing  $H$  just by a sum of density-dependent pair potentials  $u(r; \rho)$  can then lead to attractive parts in  $u(r; \rho)$  which however result from the attractive three-body term  $H_3$ . RUSS C., VAN ROIJ R. and VON GRÜNBERG H. H., submitted to *Phys. Rev. E* (2002).